Review

Polymer Electrolytes for Lithium-Sulfur Batteries: Progress and Challenges

Mingxun Jia [1], Tunan Li [1], Daotong Yang [1], Luhua Lu [2], Limei Duan [1,*], Jinghai Liu [1,*] and Tong Wu [1,*]

[1] Inner Mongolia Engineering Research Center of Lithium-Sulfur Battery Energy Storage, Inner Mongolia Key Laboratory of Carbon Nanomaterials, College of Chemistry and Materials Science, Inner Mongolia Minzu University, Tongliao 028000, China; jiamingxun23@imun.edu.cn (M.J.); litunan@imun.edu.cn (T.L.); yangdaotong23@imun.edu.cn (D.Y.)

[2] Key Laboratory of Geological Survey and Evaluation of Ministry of Education, China University of Geoscience, Wuhan 430074, China; lhlu@cug.edu.cn

* Correspondence: duanlm@imun.edu.cn (L.D.); jhliu2015@imun.edu.cn (J.L.); wutong932@imun.edu.cn (T.W.)

Abstract: The lithium-sulfur battery has garnered significant attention from both researchers and industry due to its exceptional energy density and capacity. However, the conventional liquid electrolyte poses safety concerns due to its low boiling point, hence, research on liquid electrolytes has gradually shifted towards solid electrolytes. The polymer electrolyte exhibits significant potential for packaging flexible batteries with high energy density owing to its exceptional flexibility and processability, but it also has inherent disadvantages such as poor ionic conductivity, high crystallinity, and lack of active groups. This article critically examines recent literature to explore two types of polymer electrolytes, namely gel polymer electrolyte and solid polymer electrolyte. It analyzes the impact of polymers on the formation of lithium dendrites, addresses the challenges posed by multiple interfaces, and investigates the underlying causes of capacity decay in polymer solid-state batteries. Clarifying the current progress and summarizing the specific challenges encountered by polymer-based electrolytes will significantly contribute to the development of polymer-based lithium-sulfur battery. Finally, the challenges and prospects of certain polymer solid electrolytes in lithium-sulfur battery are examined, thereby facilitating the commercialization of solid polymer electrolytes.

Keywords: polymer electrolytes; reaction kinetics; interface stability; lithium sulfur battery

1. Introduction

Addressing environmental challenges such as global warming and escalating horizontal trends, the worldwide imperative to advance deployment of carbon peak, and carbon neutrality strategic decision-making necessitates urgent efforts towards, developing high-capacity, low-cost, and environmentally-friendly green renewable energy storage devices [1–3]. Lithium-sulfur battery (LSB) exhibits a high theoretical energy density, abundant natural reserves of active material sulfur, low price, safety features, and environmental friendliness, rendering it a promising contender for the next generation of sustainable energy storage devices. However, the redox reactions involved in the charge-discharge reaction process of LSB ($S_8+16Li^++16e^- \rightleftharpoons 8Li_2S$) exhibit a high level of complex, and necessitating multiple steps for each charge-discharge process. Conventional liquid electrolyte lithium-sulfur batteries have two voltage plateaus during discharge. The first plateau corresponds to the reduction reaction of S_8 to soluble polysulfides (Li_2S_8, Li_2S_6, Li_2S_4). The second plateau corresponds to the conversion of polysulfides to insoluble short-chain sulfides (Li_2S_2, Li_2S). There is only one voltage plateau during charging, with the oxidation of short-chain sulfides to long-chain polysulfides. Long-chain lithium polysulfide serves as an intermediate product during the charge-discharge process, which is easily soluble in ether electrolyte and directly reacts with the lithium metal anode through the separator. At the same time, the active material sulfur has serious volume change during the cycle

(expansion 80%). On the other hand, the sulfur and its discharge product (Li_2S, Li_2S_2) have some inherent problems such as low conductivity and slow reaction kinetics. Among them, the shuttle effect of lithium polysulfide is a 'fatal factor' affecting the industrialization process of LSB. In order to address problems, the development of LSB must face many challenges, including irreversible loss of active material sulfur during cycling, poor cycle life, and low coulombic efficiency [4–10].

To cope with the above challenges, researchers have made a variety of attempts, for example designing and preparing high-conductivity sulfur host materials with adsorption capacity for lithium polysulfides, using the ability of materials to adsorb lithium polysulfides for separator modification and protecting the lithium metal [11–15]. The conventional commercial liquid electrolyte of LSB exhibits a high ionic conductivity, which can meet the normal working requirements of LSB. However, the presence of the complex electrochemical reactions, side reactions, and the formation of lithium dendrites during cycling inevitably, leads to a reduction in energy density for LSB. Moreover, the explosive nature of the ether electrolyte poses significant safety concerns. To address these issues, researchers have devoted considerable efforts towards developing safer alternatives. In recent years, researchers have discovered that solid electrolytes present a viable solution to aforementioned issues [16]. Solid electrolyte can be primarily classified into three categories, inorganic solid electrolyte (ISE), solid polymer electrolyte (SPE) and gel polymer electrolyte (GPE). ISEs (e.g., NASICON-type, $Li_{1.5}Al_{0.5}Ge_{1.5}(PO_4)_3$ (LAGP), garnet-type $Li_{6.4}La_3Zr_{1.4}Ta_{0.6}O_{12}$ (LLZTO), $Li_{10}GeP_2S_{12}$ and β-Li_3PS_4) exciting research finding have revealed that certain ISEs demonstrate higher ionic conductivity than liquid electrolytes even at room temperature. Despite the numerous advantages of ISEs, their reaction kinetics are hindered by excessive interfacial impedance [17–26]. The gel electrolytes exhibit high ionic conductivity of liquid electrolytes ($>10^{-3}$ S cm^{-1}) and the safety advantages of solid electrolytes. Regrettably, due to the existence of liquid electrolytes, it remains challenging to completely eliminate the detrimental impact of the polysulfide shuttle effect, leading to the capacity attenuation in battery [27–36]. The SPE exhibits favorable processability and can be modified. Regrettable, the high crystallinity at room temperature leads to the low conductivity and interface issues, the GPEs necessary to increase the temperature to maintain the normal charge-discharge of the battery and improve the poor interface contact. Researchers have proposed various strategies to ameliorate the deficiencies of GPEs.

This article reviews a comprehensive review of polymer solid electrolytes and focuses on the rational design modifications design of GPE/SPE for LSB, which are systematically discussed in terms of improving ionic conductivity and stabilizing interfaces. By discussing the issues addressed by the current strategies, the mechanism of improving ion transport rate and interface mechanical properties is clarified, while also envisioning the potential design and application of GPE/SPE in LSB (Figure 1).
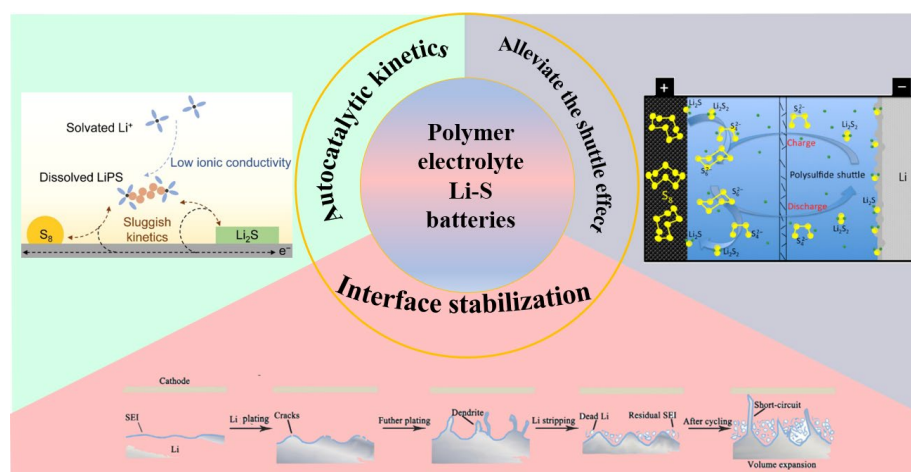
Figure 1. Polymer electrolytes for lithium-sulfur batteries: problems to be solved.

2. Classification of Polymer Electrolyte

The polymer electrolyte primarily consists of a diverse range of high molecular weight polymers as matrix materials, such as polyethylene oxide (PEO) [37,38], polyvinylidene fluoride (PVDF) [39,40], polyacrylonitrile (PAN) [41], polymethyl methacrylate (PMMA) [42], and their derivatives. The ideal polymer electrolytes should possess high ionic conductivity, excellent electrical insulation, a wide electrochemical stability window, and chemical stability when in contact with electrode materials. The electrolyte composed solely of lithium salt and polymer, in fact, falls short of meeting the above requirements. In recent years, various solutions have been reported to enhance the performance of LSB, including the crosslinking modification of polymer [43,44], the incorporation of gel polymer electrolyte by adding electrolyte [45–50], and the formation of composite polymer electrolytes by introducing inorganic materials [51–60]. The performance of the battery can be enhanced by optimizing the mechanical properties, ionic conductivity, and interface issues, however, distinct polymer electrolytes exhibit different mechanisms during charging and discharging process. According to the physical and chemical properties of various polymer electrolytes, the following classifications are made in this article.

2.1. Gel Polymer Electrolyte (GPE)

The GPE is an intermediate between liquid electrolyte and solid electrolyte form. GPEs are composed of robust host materials ensuring mechanical integrity, liquid solutions providing electrochemical properties, sometimes supplemented with fillers to enhance ionic conductivity, and an intermediate state between liquid and solid [37,41]. GPEs with high ionic conductivity of liquid electrolyte ($>10^{-3}$ S cm^{-1}) and excellent safety of solid electrolyte. The most common GPEs are polymer-based, exhibiting a sponge like structure with interconnected voids, that enable complete absorption of electrolyte, resulting in an expanded gel phase [39]. Consequently, GPE exhibits superior ionic conductivity compared to other solid electrolytes. However, in LSB the effects of the lithium polysulfide shuttle effect cannot be eliminated in the gel polymer electrolyte due to the presence of a liquid electrolyte. And owing to its complex composition, the gel polymer electrolyte encompasses multiple interface factors, including the electrode-electrolyte interface and the solid-liquid electrolyte interface. In LSB GPE still encounters challenges related to the shuttle effect and safety problems due to the presence of liquid in its components. Many excellent works have been reported, which effectively solve the above problems [43–60].

The presence of an ether bond in PEO enhances its affinity towards ether-based electrolytes, so it is easier to absorb electrolytes. The interaction between the ether bond of PEO and Li$^+$ ions establish a transfer pathway for Li$^+$ transfer. However, on account of the semi-crystalline nature of PEO, its conductivity at room temperature cannot meet the needs of LSB. The PEO segment of Aldalur et al. [43] was modified by GPE, and propylene oxide (PO) and ethylene oxide (EO) were incorporated to obtain a novel electrolyte with enhanced ionic conductivity. The results show that the coexistence of PO and EO in the polymer structure controls over its crystallization behavior while maintaining favorable interaction with Li$^+$ ions. Zhou et al. [44] reported a super ionic conductive gel polymer (SHGP) electrolyte. They designed a novel structure by grafting nitrogen-containing polyethylenimide (PEI) onto ether-like line segment polyethylene glycol diglyceride (PEGDE) to construct a GPE with high ionic conductivity. This research has significantly advanced development of gel electrolytes for LSB (Figure 2a).

In order to address the challenge of limited adsorption of LiPSs by conventional polymers, leading to the shuttle effect and subsequent capacity decay in lithium-sulfur solid-state batteries. PVDF is commonly employed as the matrix material of GPE due to its superior mechanical strength, stability, and porosity. But its ability to efficiently adsorb LiPSs is hindered by permeability of LiPSs. The sandwich structure polymer (PVDF/PMMA/PVDF) was fabricated by Yang et al. [45] through a coating process. The new polymer incorporates PVDF to enhance the adsorption of ether electrolyte and promote Li$^+$ migration, while PMMA is utilized for capturing LiPSs. By employing is the

PVDF/PMMA/PVDF separator, the shuttle effect in cycling process is availably suppressed because of the strong physical shielding and chemical absorption of the GPE (Figure 2b). The results demonstrated that the LSB with the PVDF/PMMA/PVDF separator exhibited a high initial discharge capacity, excellent electrochemical reversibility (0.18% capacity decay per cycle) and enhanced cycle stability. Song et al. [46] proposed a strategy for in situ polymerisation of liquid electrolytes using α-lipoic acid (ALA) as an additive. Due to electrochemical and chemical polymerisation a polysulfide repellent layer is formed on the positive electrode sheet. The in-situ poly-ALA layer effectively prevents the shuttle of polysulfides (as depicted in Figure 2c), thereby improving the discharge capacity and cycle stability. Han et al. [47] employed polydopamine (PDA) as an additive in PVDF, and indicating in-situ polymerization for the preparation of gel polymer additives. The presence of pyrrole nitrogen in the polydopamine structure renders it lithium-philic through Lewis acid-base interaction. This lithophilic gel polymer electrolyte plays a key role in regulating the nucleation and stripping/plating process of the lithium anode, thereby promoting the smooth surface formation of a stable SEI and ensuring long-term battery cycling. Consequently, the lithium anode interface is effectively stabilized and the electrochemical performance is improved.
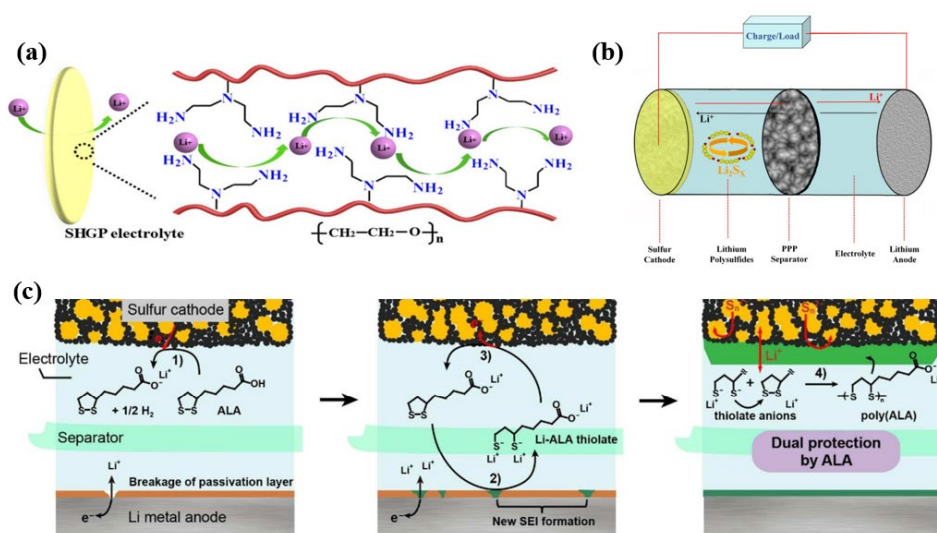
Figure 2. (**a**) The schematic illustration and the working principle of high ionic conductive SHGP gel electrolyte [44]. (**b**) Schematic configuration of the Li–S cell with PPP separator [45]. (**c**) Reaction scheme for the formation of poly (ALA) layer on the sulfur cathode and of SEI layer on lithium metal anode during the first discharge of a Li–S battery [46].

Liu et al. [48] proposed a pentaerythritol tetraacrylate (PETEA)-based GPE. This GPE is simple to prepare and has a high ionic conductivity (1.13×10^{-2} S cm^{-1}) (Figure 3a). Even when in direct contact with the bare sulfur cathode, this GPE enables the polymer lithium battery to exhibit a reduced electrode/GPE interface resistance, enhanced rate capacity (601.2 mAh g^{-1} at 1C) and improved capacity retention (81.9% after 400 cycles at 0.5C). Du et al. [49] also chose PETEA as host. The synthesis of a novel polyethylene (PE) separator supported GPE rich in ester groups was synthesized through in-situ polymerization of PETEA with divinyladipate (Ester) on the PE separator (Figure 3b). The novel GPE exhibits a notable ionic conductivity of 2.8×10^{-4} S cm^{-1} at room temperature, along with an extensive electrochemical stability window of 4.75 V vs. Li/Li$^+$. This in-situ growth method on the separator facilitates enhanced the electrolyte-electrode contact, which can effectively solve the interface problem. Du et al. assembled a lithium-sulfur flexible pack battery in order to validate a flexible gel polymer electrolyte, and showed that an orange light-emitting diode lamp could be lit after several folds and the voltage was around 2.5 V (Figure 3c). However, the majority of in-situ polymerization processes lack spontaneity

and necessitate the presence of initiators, thereby introducing uncertainty into battery performance. The utilization of lithium salts as initiators for in-situ polymerization can effectively address the issue of adding additional initiators to the battery system. Yang et al. [50]. employed lithium hexafluorophosphate as an in-situ polymerization initiator for the synthesis of 1,3-dioxolane (PDXL) through DOL polymerization. And the PVA-CN was introduced into the matrix to establish an interpenetrating network (IPN) though in-situ cross-linking on the cathode side (Figure 3d). This method not only circumvents the need of introduction for additional initiators, but also facilitates uniform lithium deposition though utilization of PDXL-GPE on the anode side. The LSB with the asymmetric PDXL-GPE demonstrate excellent electrochemical performance, retaining a capacity of 807 mAh g^{-1} after 500 cycles at 0.5C and high coulombic efficiency.
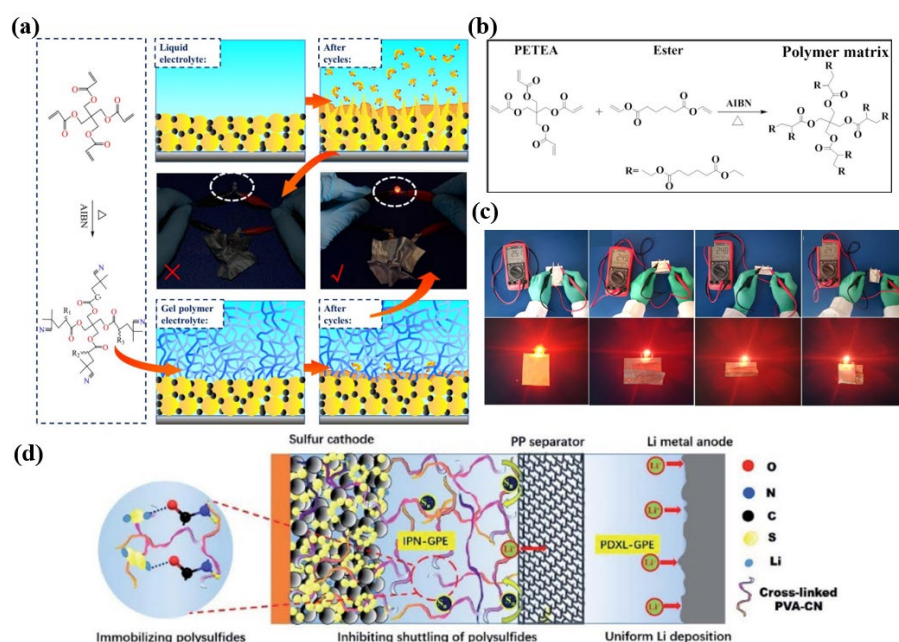
Figure 3. (**a**) The schematic illustration and the working principle of high ionic conductive PETEA-based GPE [48]. (**b**)The schematic diagram of polymerization mechanism for the polymer matrix of PEGPE. (**c**) Open-circuit voltage of a soft packed Li-S battery and photos of an orange LED lamp powered by the soft packed Li-S battery under various states [49]. (**d**) Schematic diagram of the Li-IPN-GPE-S battery with the asymmetric GPE network [50].

The aforementioned modification methods of gel electrolytes for LSB effectively enhance interface contact, mitigate impedance problems, and improve lithium deposition. The mechanical stability and rigidity of the gel polymer have a direct effect on the inhibition of dendrite growth, which is an intriguing observation. The introduction of inorganic nanoparticles (e.g., TiO_2 [51–53], Al_2O_3 [54], and SiO_2 [55–58]) into the polymer matrix will enhance the GPE rigidity and can effectively solve this problem. Pei et.al. [59] designed and synthesised titanium oxide clusters (TOC) for GPE enhancement in order to prepare low E/S LSB that are more suitable for industrialization Metal oxide clusters represent a significant category of organic-inorganic hybrid materials, which can improve the mechanical and electrochemical properties of GPE. Poly (vinylidene fluoride-co-hexafluoropropylene) (PVFH) was employed as the polymer matrix in this study. Inorganic-organic composite gel electrolyte was prepared by mixing TOC and polyethylene glycol (PEG) (Figure 4a). The results demonstrate that surface modification with TOC is essential to improve the performance of GPE. Scanning electron microscopy was used to characterize the lithium metal of LSB after cycling. The effective inhibition of dendrite growth and protection of lithium metal by PVFH-TOC-PEG. Xie et al. [60] designed a novel composite gel polymer electrolyte using PEO and PAN as substrates doped with LLZO (Figure 4b). The combina-

tion of PAN and PEO can effectively integrate the favorable mechanical properties inherent in PEO with the excellent ionic conductivity exhibited by PAN. The introduction of LLZO can effectively improve the mechanical properties of the composites, thereby promoting the utilization efficiency of elemental sulfur and improving the long-term cycling stability as well as rate capability of LSB. The electrochemical properties of some reported GPE for LSB are presented in Table 1.
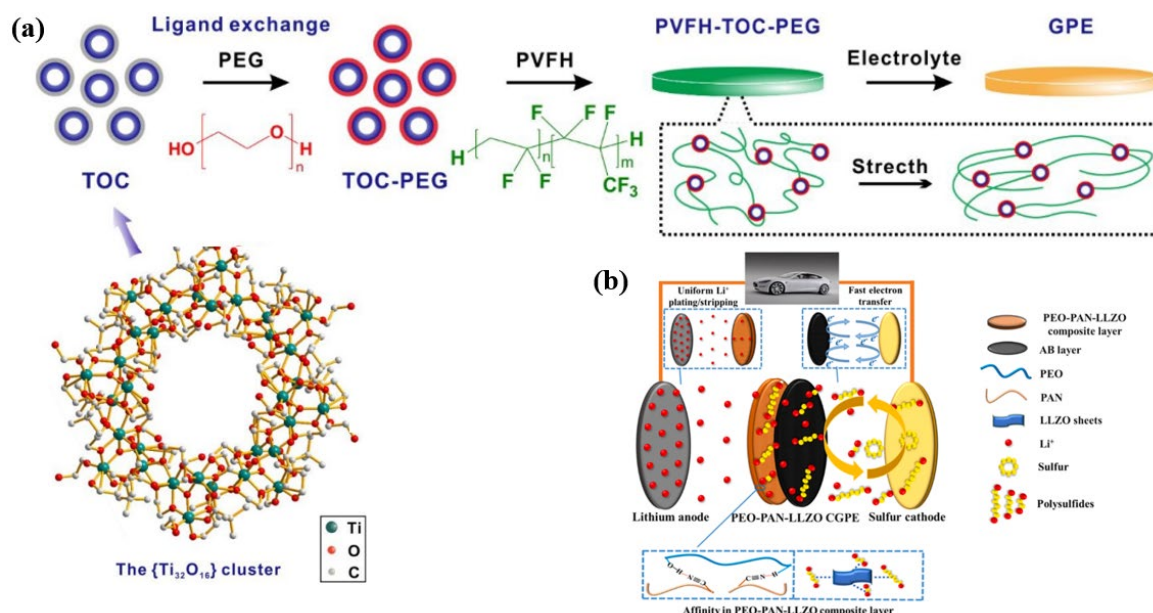

Figure 4. (**a**) Crystal structure of TOC and schematic illustration for the synthesis of the PVFH-TOC-PEG electrolyte [59]. (**b**) Schematic illustration for the performance improvement mechanisms of PEO-PAN-LLZO CGPE applied in the Li-S battery [60].

Table 1. The electrochemistry properties and advantages of GPE for LSB are mentioned in this article.

Type	Materials	Liquid Electrolyte	Conductivity	Specific Discharge Capacity	Advantages	Refs.
PEGDE	PEGDE/PEI	DOL/DME + 1 M LiTFSI	0.75×10^{-3} S cm^{-1} at 30 °C or 2.2×10^{-3} S cm^{-1} at 60 °C	950 mAh g^{-1} (0.2 C)	high ionic conductivity adsorbable LiPSs high capacity retention rate	[44]
PVDF	PMMA	DOL/DME + 1 M LiTFSI	1.95×10^{-3} S cm^{-1} at RM	1711.8 mAh g^{-1} (0.1 C)	high initial discharge capacity high capacity retention rate	[45]
PVDF	PDA	DOL/DME + 1 M LiTFSI	-	1215.4 mAh g^{-1} (0.1 C)	high capacity retention rate protect lithium anode	[47]
PETEA	AIBN	DOL/DME + 1 M LiTFSI + 1 wt% LiNO$_3$	1.13×10^{-2} S cm^{-1} at RM	1219.8 mAh g^{-1} (0.1 C)	high ionic conductivity high flexibility protect lithium anode	[48]
DOL(PDXL)	PVA-CN	DOL/DME + 1 M LiTFSI	3.23×10^{-3} S cm^{-1} at RM	1130 mAh g^{-1} (0.1 C)	promote lithium deposition long cycle stability	[50]
PVFH	TOC/PEG	DOL/DME + 1 M LiTFSI + 2 wt% LiNO$_3$	8×10^{-3} S cm^{-1} at RM	1103 mAh g^{-1} (0.1 C)	support low E/S ratio and low N/P ratio. high cycling stability	[59]
PEO/PAN	LLZO	DOL/DME + 1 M LiTFSI + 1 wt% LiNO$_3$	2.01×10^{-3} S cm^{-1} at RM	1459 mAh g^{-1} (0.1 C)	good interface stability long cycle stability	[60]

2.2. Solid Polymer Electrolyte (SPE)

In recent years, all-solid-state lithium-sulfur batteries (ASSLSB) have garnered increased attention due to their potential in preventing the shuttle effect, inhibiting dendrite growth, and providing high flame retardancy [61–65]. Compared to other solid inorganic electrolytes, polymer-based solid-state electrolytes exhibit several advantages. Firstly, they exhibit excellent machinability and can be easily modified, though the incorporation of inorganic additives and deposition of ultra-thin films. Secondly, they exhibit superior adhesion properties, ensuring optimal interface contact, and accommodating the volume change of the electrode. The drawback of polymer-based solid electrolyte, lies in their relatively low ionic conductivity, insufficient ability to inhibit the shuttle effect, and inadequate mechanical properties for inhibiting the growth of Li dendrites when without the addition of electrolyte [66–71]. The charge and discharge process of solid polymer LSB was monitored in real-time using an optical microscope by Song et al. [72]. The solid polymers in this study were based on PEO with the addition of LLZTO and LiTFSI. The monitoring results show that the electrolyte undergoes an irreversible color change from bright white to dark brown during the charge and discharge reaction. This phenomenon indicates the occurrence of shuttle reaction involving polysulfides with in the solid electrolyte (Figure 5). Simultaneously, the researchers acquired the identical observations through XPS and Raman analysis. The same experiments and tests were carried out by adjusting the temperature. The experimental result revealed that variations in temperature exerted a significant influence on the shuttle of solid electrolyte polysulfide, corrosion of lithium metal, and expansion of the positive electrode. Consequently, these factors contributed to a decline in the electrochemical performance of the battery. In order to address the above issues, researchers have reported various strategies to overcome them, such as introducing lithium salt additives and inorganic fillers into different polymers matrices fabricate all-solid-state polymer lithium-sulfur batteries. These strategies effectively overcome the limitations of polymer electrolytes by providing a comprehensive, understanding of ion conduction mechanism, reaction process, anode and cathode interfaces, as well as interactions between polymer and inorganic fillers.
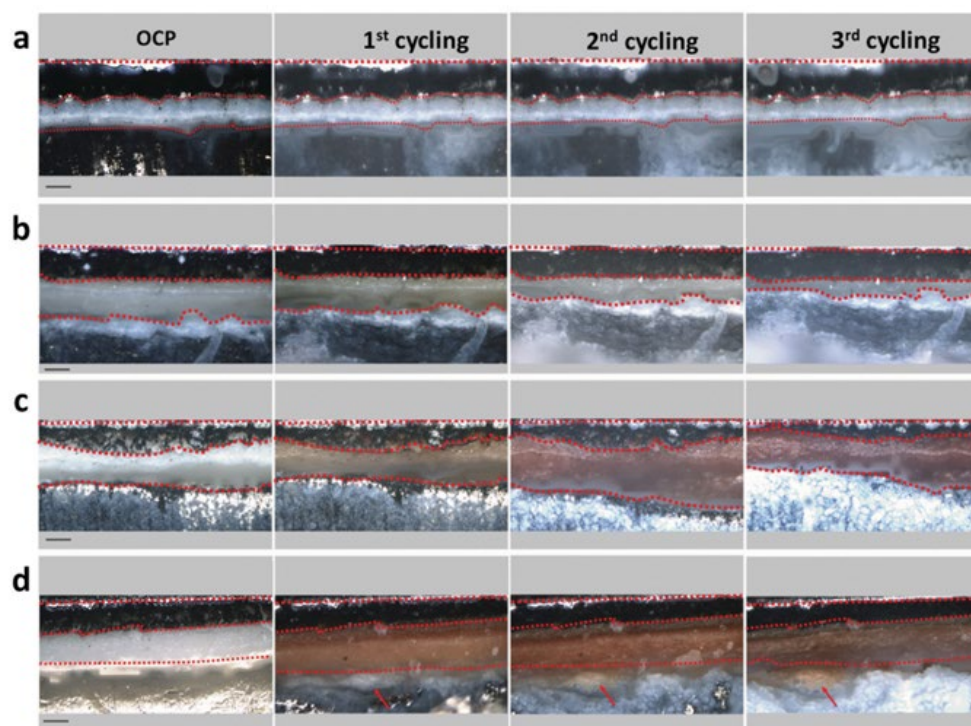
Figure 5. In situ OM imaging of ASSLS batteries at (**a**) 45 °C, (**b**) 55 °C, (**c**) 65 °C and (**d**) 75 °C for OCP and after the first, second and third discharge–charge cycles, respectively [72].

The SPE is solvent-free material that conducts electricity only by ions in a polar polymer network, where in the dissociation of lithium salts occur within polar polymers, facilitating the continuous extraction/intercalation of Li^+ ions and providing ionic conductivity. The PEO substrate is widely employed in SPE due to its high ionic conductivity, strong solvation ability of ethylene oxide (EO) units, and high electrochemical stability. Unfortunately, the ionic conductivity of PEO with lithium salt at room temperature still falls significantly short of that exhibited by liquid electrolyte, necessitating the operation of PEO-based SPEs at temperatures above 60 °C (semi-melting). The transfer of Li^+ ions is achieved through the movement of fragment between coordination sites and the hopping of ions within and between chains [73,74]. Enhancing ionic conductivity can be effectively achieved by manipulating segmental motion through temperature elevation or reduction of the glass transition temperature.

The cycling process of LSB in liquid electrolyte and gel electrolyte primarily relies on the conduction within the liquid phase. However, in the SPE, such as PEO, the operational mechanism of LSB undergoes significant alterations. The PEO exhibits excellent LiPSs dissolution capability owing to the high donor number (DN) of its ethylene oxide unit, which also contributes to its strong solvation ability for lithium salts. Moreover, the electrochemical reaction of mechanism PEO-based electrolyte closely resembles that of liquid ether-based lithium-sulfur battery. Consequently, the shuttle effect will also impact the PEO-based electrolyte in LSB. Marceau et al. [75] study was different from conventional performance testing studies. Them employed scanning electron microscopy and ultraviolet absorption spectroscopy to investigate the charge and discharge process of a LSB with crosslinked polyethylene oxide as the polymer solid electrolyte. The observation results demonstrate that during the charging process of LSB, the dissolution of various polysulfides in the solid polymer electrolyte facilitates the formation of an insulating sulfur-rich layer on the surface of the metal lithium. The appearance of elemental sulfur during charge reaction at a voltage equal to or exceed in 2.3 V, and the reduction in thickness of SPE upon cycling. The formation of S_4^{2-} during discharge and S_6^{2-} during charging has been identified as the primary factors to the distinct mechanisms observed in the charging and discharging processes. The high solubility of S_4^{2-} and S_6^{2-} leads to anodic passivation and redox shuttling. Although the shuttle effect of polysulfides persists in the PEO system of LSB, its magnitude is significantly attenuated compared to that observed in liquid electrolyte. Solid thin film polymer electrolytes offer a promising solution by mitigating the intricate dynamics associated with polysulfide equilibria. Consequently, polymer electrolytes have garnered considerable attention among researchers.

The formation of soluble polysulfides was effectively inhibited by Fang et al. [76] through the application of a polyvinylidene fluoride (PVDF) coating on the sulfur cathode in PEO-based LSB. Furthermore, they successfully altered the reaction mechanism for sulfur from a multi-step 'solid-liquid-solid' reaction to a single-step 'solid-solid' reaction. Due to the insolubility and instability of long-chain polysulfides in low-solvent PVDF polymers, this approach facilitates direct conversion of elemental sulfur into solid Li_2S_2/Li_2S without intermediate products formation. However, the strong attraction of PEO-Li_2Sn (n = 4–8) leads to the dissolution of polysulfides within the PEO matrix. This approach of solving the shuttle effect caused by polysulfides from the source significantly improves the electrochemical performance. Sheng et al. [77] designed a SPE based on PEO containing ionic liquid grafted oxide nanoparticles (IL @ NPs). And doped with designed ZrO_2, TiO_2 and SiO_2 to compare their electrochemical properties. The results demonstrate that the electrolyte containing IL @ ZrO_2 exhibits the highest ionic conductivity at 50 °C and 37 °C, with values of 4.95×10^{-4} and 2.32×10^{-4} S cm^{-1}, respectively. The electrochemical performance in LSB is improved, enabling the delivery of a high specific capacity of 986 mAh g^{-1} and 600 mAh g^{-1} can be provided at 50 °C and 37 °C, respectively.

Wei et al. [78] employed fullerene (C_{60}) as additive in the solid polymer electrolyte for LSB and conducted a comprehensive investigation of its properties (Figure 6a). Due to the π-bent surface of C_{60}, the ionic conductivity of PEO is increased to 1.27×10^{-4} S cm^{-1}

at 60 °C by increasing the migration of the chain segments and dissociating the ionic binding of LiTFSI due to easier interactions with the n-orbitals of the PEO ether oxygen atoms. The interface problem has been effectively addressed with the addition of C_{60}. PEO-C_{60} demonstrates remarkable capability in inhibiting the growth and penetration of Li dendrites, thus ensuring a stable cycle durability of 1000 h in lithium symmetric cell. Liu et al. [79] also chose Nb_2CT_x MXene with high conductivity as the inorganic filler for PEO. Research findings have demonstrated that the specific surface area-related penetration effect of Nb_2CT_x MXene significantly influences Li^+ ions conductivity and polysulfide adsorption. The ionic conductivity of PEO electrolyte was observed to increase to 2.62×10^{-4} S cm^{-1} when the sheet size of Nb_2CT_x MXene size was adjusted below 100 nm by adjusting. The migration number of improved Li^+ ions at 60 °C is determined to be 0.37. When incorporated into an all-solid-state Lithium-sulfur battery at a rate of 0.5C, the initial capacity was 1149 mAh g^{-1} and the capacity remained 491 mAh g^{-1} after 200 cycles, demonstrating excellent cycling performance. Zhang et al. [80] employed In_2O_3 as a multifunctional nanofiller in the PEO matrix. The nano-In_2O_3 not only improves the ionic conductivity of PEO electrolyte but also facilitates the formation of an in-situ Li-In alloy layer at the interface between the electrolyte and anode. The alloy layer effectively protects the lithium metal and achieves the effect of inhibiting the shuttle effect. It shows excellent cycle stability (exceeding 1200 h) in symmetric lithium batteries.
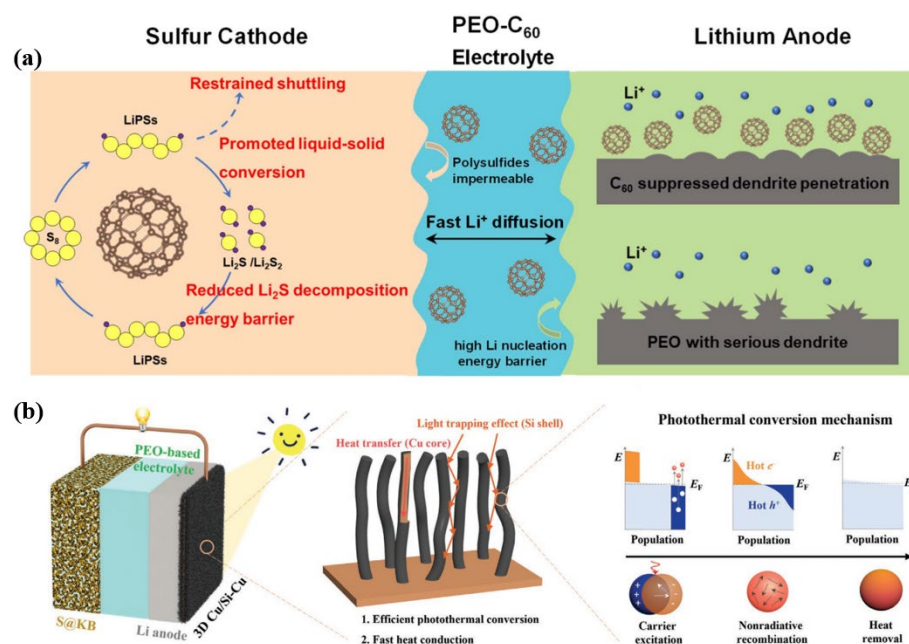
Figure 6. (**a**) Schematic illustration of the configuration and merits of all solid-state lithium–sulfur batteries with the PEO-1% C_{60} solid polymer electrolyte [78]. (**b**) The structure diagram, working process and corresponding photothermal conversion mechanism of 3D Cu/SiCu nanowire-based room temperature polymer ASSLSB [81].

In addition to this direct method of improving the solid electrolyte, Wang et al. [81] proposed an innovative photothermal battery technology that can effectively work at room temperature. The researchers synthesized a three-dimensional Cu substrate featuring a Cu/Si core-shell structure, which was positioned between the lithium anode and the glass shell. The non-radiative recombination of the Si nanoshell facilitates efficient light to enter and effectively generate heat. (Figure 6b) The heat is rapidly transferred to the battery system via the Cu core, facilitating exceptional reaction kinetics and photothermal conversion performance under simulated and real sunlight conditions. Song et al. [82] also demonstrated the utilization of copper-silicon nanowires in a wide-temperature solid-state polymer electrolyte lithium-sulfur battery. The researchers achieved heat conversion through a

layered copper-silicon nanowire photothermal current collector, which exhibits efficient photothermal conversion. This current collector enhances the charge storage and transport of the electrode/electrolyte system and its interface even under low operating temperatures. In the LSB with $Li_{1.5}Al_{0.5}Ge_{1.5}P_3O_{12}$ (LAGP) electrolyte, PEO electrolyte and LiTFSI electrolyte, the discharge capacity is 900 mAh g^{-1} at room temperature, 960 mAh g^{-1} at 60 °C and 260 mAh g^{-1} at −60 °C. In the study conducted by Li et al. [83], sulfurized polyacrylonitrile (S/PAN) was employed as a substitute for the conventional S/C as the cathode in the solid electrolyte, while $Li_{3.25}Ge_{0.25}P_{0.75}S_4$ (LGPS) was introduced into the PEO-based electrolyte to replace traditional rigid inorganic solid electrolyte particles. The results demonstrate that the introduction of LGPS can effectively improve the wettability of polymer electrolyte and reduce charge transfer resistance. The aforementioned approach, involving the introduction of inorganic fillers into PEO-based electrolytes, significantly improves mechanical strength to achieve the purpose of regulating the interface of lithium dendrite inhibition. Therefore, the incorporation of inorganic particles into the polymer electrolyte is a highly effective approach to improve the mechanical properties, while simultaneously expanding the base voltage window within the working temperature range. The good contact between the polymer electrolyte and the positive electrode plays a pivotal role in determining both the Coulombic efficiency and rate performance of the batteries. The density disparity between sulfur and Li_2S results in a fluctuation of the positive electrode volume during the battery charging and discharging, that directly impacts cycle performance and sulfur utilization. Marceau et al. [75] observed the cathode morphology of a solid polymer lithium-sulfur battery after cycling by SEM and EDS analysis. It was observed that, the cathode morphology underwent changes and the distribution of sulfur became uneven. The capacity decay coulombic efficiency of the battery performance is reduced as a result, necessitating reasonable control of the mechanical properties of the electrolyte in addressing interface issues for designing a reasonable solid polymer lithium sulfur battery. It is crucial to strike a balance between sufficient rigidity to suppress dendrite formation and adequate flexibility to accommodate the cathode.

In addition to this approach of introducing inorganic fillers for improve conductivity, alternative strategies have been employed by researchers. Zhong et al. [84] achieved varying degrees of crosslinking in the SPEs by controlling the monomer ratio, resulting in slightly crosslinked SCP (sc-SCP) membranes that inhibited the shuttle of LiPSs within the sulfur cathode and highly crosslinked SCP (hc-SCP) membranes that improved the mechanical strength of the membrane. By adjusting the position and chemical structure of the SCP and EO segments, Zhong et.al. successfully enhance both storage modulus, and ionic conductivity while simultaneously the improving the interface stability of the lithium anode through an artificial SEI layer. Consequently, LiPSs dissolve without undergoing shuttling phenomena, thereby imparting the cell with a high capacity and retention rate. In addition to PEO-based polymer electrolytes, PVDF-based electrolytes exhibit great potential in enabling the of flexible batteries with high energy density owing to their excellent flexibility and processability. Chen et al. [40] employed cellulose acetate as matrix and bi-grafted polysiloxane copolymer, LiTFSI and PVDF as raw materials to prepare a polymer electrolyte. This approach obtained a solid electrolyte with ideal ionic conductivity and superior mechanical properties thereby effectively improving the electrochemical performance of LSB. Li-Nafion is characterized by flexibility and light weight. Due to its excellent electrical conductivity and non-electron transmission characteristics, it can be used as a solid electrolyte and a separator for solid lithium sulfur batteries. Gao et al. [85] by using the Li-Nafion membrane swollen with propylene carbonate (PC-Li-Nafion membrane) as electrolyte and separator. Due to its special construction, it acts as both a solid electrolyte and a binder, while achieving the balance of ionic and electronic conductivity, it also improves the interface contact and further improves the specific capacity. The electrochemical properties of some reported SPE for LSB are presented in Table 2.

Table 2. The electrochemistry properties and advantages of SPE for LSB are mentioned in this article.

Type	Materials	Conductivity	Specific Discharge Capacity	Advantages	Refs.
PEO	PVDF	-	825 mAh g^{-1} (0.05 C)	long cycle stability high capacity retention rate	[76]
EO	IL@NPs/ZrO$_2$	4.95×10^{-4} S cm^{-1} at 50 °C or 2.32×10^{-4} S cm^{-1} at 37 °C	986 mAh g^{-1}	high ionic conductivity	[77]
PEO	C$_{60}$	1.27×10^{-4} S cm^{-1} at 60 °C	1125 mAh g^{-1} (0.1 C)	long cycle stability inhibit dendritic	[78]
PEO	Nb$_2$CTx MXene	2.63×10^{-4} S cm^{-1} at 60 °C	1149 mAh g^{-1} (0.5 C)	long cycle stability high ionic conductivity	[79]
PEO	In$_2$O$_3$	-	1227 mAh g^{-1} (0.2 C)	long cycle stability inhibit dendritic	[80]
PVDF-HFP	DMF	7.87×10^{-3} S cm^{-1} at 60 °C	1089 mAh g^{-1} (0.2 C)	high ionic conductivity	[81]
PEO	LGPS	0.42×10^{-3} S cm^{-1} at RM	1183 mAh g^{-1} (0.2 C)	high ionic conductivity high initial discharge capacity	[83]
Li-Nafion	PC	2.1×10^{-4} S cm^{-1} at 70 °C	1072.8 mAh g^{-1} (0.05 C)	high capacity retention rate	[85]

3. Conclusions and Perspectives

All-solid-state lithium-sulfur battery is widely regarded as the most promising high-energy density storage for the next generation. However, challenges related to interface issues and slow redox kinetics impede its commercialization feasibility. Reasonable design of polymer electrolyte for regulating interface-enhanced redox kinetics can effectively addres the above issues. In recent years, researchers have proposed numerous solutions to improve the ionic conductivity, ranging from overcoming the limitations of single component materials in solid electrolytes to developing multifunctional composite catalytic materials capable of adjusting interface. The aforementioned approaches can effectively improve the overall performance of all-solid-state polymer lithium-sulfur batteries. Although great progress has been made in the design of polymer solid electrolytes, the performance of the required polymer electrolytes that can inhibit the growth of lithium dendrites while adhering to the cathode is still unclear. It is necessary to combine in-situ characterization technology with a well-established theoretical system to further explore the mechanical properties of polymer electrolytes, thereby addressing the inherent problems in the cycling process of LSB. In the future, the design of polymer electrolyte lithium-sulfur batteries should primarily focus on implementing strategies that have been proposed to improve the ionic conductivity. (1) The combination of in-situ characterization and density functional calculations enables a comprehensive understanding and validation of the instantaneous changes occurring in lithium polysulfides and catalytic materials. (2) Exploring novel organic functional groups and inorganic additives to regulate the electrode interface, while further developing catalytic materials with optimal mechanical strength matching both electrodes and accelerating the redox reaction kinetics and exploring its mechanism of action. (3) Continuously advance development of a solid-state lithium-sulfur battery system capable of supporting long-cycling and high-sulfur loading conditions, thereby facilitating industrialization and further increase the energy density of LSB. In summary, the catalytic process of the unique electrochemical reaction of solid-state lithium-sulfur batteries is deeply explored, and advanced characterization techniques are used to clarify the mechanism of eliminating the influence of interface problems on the electrochemical

performance of batteries. These findings offer valuable insights towards advancing the commercialization of LSB.

References

1. Basar, S.; Tosun, B. Environmental Pollution Index and economic growth: Evidence from OECD countries. *Environ. Sci. Pollut. Res. Int.* **2021**, *28*, 36870–36879. [CrossRef] [PubMed]
2. Fretz, S.J.; Pal, U.; Girard, G.M.A.; Howlett, P.C.; Palmqvist, A.E.C. Lithium Sulfonate Functionalization of Carbon Cathodes as a Substitute for Lithium Nitrate in the Electrolyte of Lithium–Sulfur Batteries. *Adv. Funct. Mater.* **2020**, *30*, 2002485. [CrossRef]
3. Li, C.; Ge, W.; Qi, S.; Zhu, L.; Huang, R.; Zhao, M.; Qian, Y.; Xu, L. Manipulating Electrocatalytic Polysulfide Redox Kinetics by 1D Core–Shell Like Composite for Lithium–Sulfur Batteries. *Adv. Energy Mater.* **2022**, *12*, 2103915. [CrossRef]
4. Zhang, T.; Zhang, L.; Hou, Y. MXenes: Synthesis strategies and lithium-sulfur battery applications. *eScience* **2022**, *2*, 164–182. [CrossRef]
5. Feng, L.; Yu, P.; Fu, X.; Zhang, Z.M.; Davey, K.; Wang, Y.; Guo, Z.; Yang, W. Regulating Polysulfide Diffusion and Deposition via Rational Design of Core-Shell Active Materials in Li-S Batteries. *ACS Nano* **2022**, *16*, 7982–7992. [CrossRef] [PubMed]
6. Zhang, C.Y.; Zhang, C.; Pan, J.L.; Sun, G.W.; Shi, Z.; Li, C.; Chang, X.; Sun, G.Z.; Zhou, J.Y.; Cabot, A. Surface strain-enhanced MoS_2 as a high-performance cathode catalyst for lithium–sulfur batteries. *eScience* **2022**, *2*, 405–415. [CrossRef]
7. Ji, L.; Wang, X.; Jia, Y.; Qin, X.; Sui, Y.; Yan, H.; Niu, Z.; Liu, J.; Zhang, Y. Oxygen and nitrogen tailoring carbon fiber aerogel with platinum electrocatalysis interfaced lithium/sulfur (Li/S) batteries. *Chin. Chem. Lett.* **2023**, *34*, 107123. [CrossRef]
8. Wang, Z.; Ge, H.; Liu, S.; Li, G.; Gao, X. High-Entropy Alloys to Activate the Sulfur Cathode for Lithium–Sulfur Batteries. *Energy Environ. Mater.* **2022**, *6*, e12358. [CrossRef]
9. Wang, B.; Wang, L.; Zhang, B.; Zeng, S.; Tian, F.; Dou, J.; Qian, Y.; Xu, L. Niobium Diboride Nanoparticles Accelerating Polysulfide Conversion and Directing Li_2S Nucleation Enabled High Areal Capacity Lithium-Sulfur Batteries. *ACS Nano* **2022**, *16*, 4947–4960. [CrossRef]
10. Zhang, H.; Ono, L.K.; Tong, G.; Liu, Y.; Qi, Y. Long-life lithium-sulfur batteries with high areal capacity based on coaxial $CNTs@TiN-TiO_2$ sponge. *Nat. Commun.* **2021**, *12*, 4738. [CrossRef]
11. Xue, P.; Zhu, K.; Gong, W.; Pu, J.; Li, X.; Guo, C.; Wu, L.; Wang, R.; Li, H.; Sun, J.; et al. "One Stone Two Birds" Design for Dual-Functional TiO_2-TiN Heterostructures Enabled Dendrite-Free and Kinetics-Enhanced Lithium–Sulfur Batteries. *Adv. Energy Mater.* **2022**, *12*, 2200308. [CrossRef]
12. Li, Z.; Sami, I.; Yang, J.; Li, J.; Kumar, R.V.; Chhowalla, M. Lithiated metallic molybdenum disulfide nanosheets for high-performance lithium–sulfur batteries. *Nat. Energy* **2023**, *8*, 84–93. [CrossRef]
13. Xu, J.; Xu, L.; Zhang, Z.; Sun, B.; Jin, Y.; Jin, Q.; Liu, H.; Wang, G. Heterostructure $ZnSe-CoSe_2$ embedded with yolk-shell conductive dodecahedral as Two-in-one hosts for cathode and anode protection of Lithium–Sulfur full batteries. *Energy Storage Mater.* **2022**, *47*, 223–234. [CrossRef]
14. Wu, T.; Ye, J.; Li, T.; Liu, Y.; Jia, L.; Sun, L.; Liu, J.; Xie, H. Tetrathiafulvalene as a multifunctional electrolyte additive for simultaneous interface amelioration, electron conduction, and polysulfide redox regulation in lithium-sulfur batteries. *J. Power Sources* **2022**, *536*, 231482. [CrossRef]
15. Wu, T.; Sun, G.; Lu, W.; Zhao, L.; Mauger, A.; Julien, C.M.; Sun, L.; Xie, H.; Liu, J. A polypyrrole/black-TiO_2/S double-shelled composite fixing polysulfides for lithium-sulfur batteries. *Electrochim. Acta* **2020**, *353*, 136529. [CrossRef]
16. De Luna, Y.; Abdullah, M.; Dimassi, S.N.; Bensalah, N. All-solid lithium-sulfur batteries: Present situation and future progress. *Ionics* **2021**, *27*, 4937–4960. [CrossRef]
17. AbdelHamid, A.A.; Cheong, J.L.; Ying, J.Y. Metal oxide-mediated differential chalcogen morphogenesis for Li-chalcogen battery application. *Nano Energy* **2021**, *84*, 105842. [CrossRef]

18. Pervez, S.A.; Vinayan, B.P.; Cambaz, M.A.; Melinte, G.; Diemant, T.; Braun, T.; Karkera, G.; Behm, R.J.; Fichtner, M. Electrochemical and compositional characterization of solid interphase layers in an interface-modified solid-state Li–sulfur battery. *J. Mater. Chem. A* **2020**, *8*, 16451–16462. [CrossRef]

19. Yan, C.; Zhou, Y.; Cheng, H.; Orenstein, R.; Zhu, P.; Yildiz, O.; Bradford, P.; Jur, J.; Wu, N.; Dirican, M.; et al. Interconnected cathode-electrolyte double-layer enabling continuous Li-ion conduction throughout solid-state Li-S battery. *Energy Storage Mater.* **2022**, *44*, 136–144. [CrossRef]

20. Lu, Y.; Huang, X.; Song, Z.; Rui, K.; Wang, Q.; Gu, S.; Yang, J.; Xiu, T.; Badding, M.E.; Wen, Z. Highly stable garnet solid electrolyte based Li-S battery with modified anodic and cathodic interfaces. *Energy Storage Mater.* **2018**, *15*, 282–290. [CrossRef]

21. Huang, X.; Liu, C.; Lu, Y.; Xiu, T.; Jin, J.; Badding, M.E.; Wen, Z. A Li-Garnet composite ceramic electrolyte and its solid-state Li-S battery. *J. Power Sources* **2018**, *382*, 190–197. [CrossRef]

22. Jin, Y.; Liu, K.; Lang, J.; Jiang, X.; Zheng, Z.; Su, Q.; Huang, Z.; Long, Y.; Wang, C.A.; Wu, H.; et al. High-Energy-Density Solid-Electrolyte-Based Liquid Li-S and Li-Se Batteries. *Joule* **2020**, *4*, 262–274. [CrossRef]

23. Wan, H.; Cai, L.; Han, F.; Mwizerwa, J.P.; Wang, C.; Yao, X. Construction of 3D Electronic/Ionic Conduction Networks for All-Solid-State Lithium Batteries. *Small* **2019**, *15*, e1905849. [CrossRef] [PubMed]

24. Nagao, M.; Hayashi, A.; Tatsumisago, M. Sulfur–carbon composite electrode for all-solid-state Li/S battery with $Li_2S–P_2S_5$ solid electrolyte. *Electrochim. Acta* **2011**, *56*, 6055–6059. [CrossRef]

25. Nagao, M.; Hayashi, A.; Tatsumisago, M. High-capacity Li_2S–nanocarbon composite electrode for all-solid-state rechargeable lithium batteries. *J. Mater. Chem.* **2012**, *19*, 10015–10020. [CrossRef]

26. Zhang, Y.; Chen, K.; Shen, Y.; Lin, Y.; Nan, C.-W. Synergistic effect of processing and composition x on conductivity of xLi_2S-$(100-x)P_2S_5$ electrolytes. *Solid State Ion.* **2017**, *305*, 1–6. [CrossRef]

27. Chen, R.; Li, Q.; Yu, X.; Chen, L.; Li, H. Approaching practically accessible solid-state batteries: Stability issues related to solid electrolytes and interfaces. *Chem. Rev.* **2019**, *120*, 6820–6877. [CrossRef]

28. Liu, G.; Sun, Q.; Li, Q.; Zhang, J.; Ming, J. Electrolyte issues in lithium–sulfur batteries: Development, prospect, and challenges. *Energy Fuels* **2021**, *35*, 10405–10427. [CrossRef]

29. Wang, C.; Zhang, X.W.; Appleby, A.J. Solvent-free composite PEO-ceramic fiber/mat electrolytes for lithium secondary cells. *J. Electrochem. Soc.* **2004**, *152*, A205. [CrossRef]

30. Yu, J.; Kwok, S.C.; Lu, Z.; Effat, M.B.; Lyu, Y.Q.; Yuen, M.M.; Ciucci, F. A ceramic-PVDF composite membrane with modified interfaces as an ion-conducting electrolyte for solid-state lithium-ion batteries operating at room temperature. *ChemElectroChem* **2018**, *5*, 2873–2881. [CrossRef]

31. Kachmar, A.; Carignano, M.; Laino, T.; Iannuzzi, M.; Hutter, J. Mapping the free energy of lithium solvation in the Protic ionic liquid ethylammonuim nitrate: A metadynamics study. *ChemSusChem* **2017**, *10*, 3083–3090. [CrossRef]

32. Prasanth, R.; Aravindan, V.; Srinivasan, M. Novel polymer electrolyte based on cob-web electrospun multi component polymer blend of polyacrylonitrile/poly (methyl methacrylate)/polystyrene for lithium ion batteries—Preparation and electrochemical characterization. *J. Power Sources* **2012**, *202*, 299–307. [CrossRef]

33. Liang, B.; Tang, S.; Jiang, Q.; Chen, C.; Chen, X.; Li, S.; Yan, X. Preparation and characterization of PEO-PMMA polymer composite electrolytes doped with nano-AlO. *Electrochim. Acta* **2015**, *169*, 334–341. [CrossRef]

34. Lu, Y.; Tu, Z.; Archer, L.A. Stable lithium electrodeposition in liquid and nanoporous solid electrolytes. *Nat. Mater.* **2014**, *13*, 961–969. [CrossRef] [PubMed]

35. Song, S.; Qin, X.; Ruan, Y.; Li, W.; Xu, Y.; Zhang, D.; Thokchom, J. Enhanced performance of solid-state lithium-air batteries with continuous 3D garnet network added composite polymer electrolyte. *J. Power Sources* **2020**, *461*, 228146. [CrossRef]

36. Han, X.; Gong, Y.; Fu, K.K.; He, X.; Hitz, G.T.; Dai, J.; Hu, L. Negating interfacial impedance in garnet-based solid-state Li metal batteries. *Nat. Mater.* **2016**, *16*, 572–579. [CrossRef] [PubMed]

37. Li, W.; Pang, Y.; Zhu, T.; Wang, Y.; Xia, Y. A gel polymer electrolyte based lithium-sulfur battery with low self-discharge. *Solid State Ion.* **2018**, *318*, 82–87. [CrossRef]

38. Nagajothi, A.J.; Kannan, R.; Rajashabala, S. Studies on electrochemical properties of poly (ethylene oxide)-based gel polymer electrolytes with the effect of chitosan for lithium–sulfur batteries. *Polym. Bull.* **2017**, *74*, 4887–4897. [CrossRef]

39. Hao, X.; Wenren, H.; Wang, X.; Xia, X.; Tu, J. A gel polymer electrolyte based on PVDF-HFP modified double polymer matrices via ultraviolet polymerization for lithium-sulfur batteries. *J. Colloid Interface Sci.* **2020**, *558*, 145–154. [CrossRef]

40. Chen, L.; Fan, L.Z. Dendrite-free Li metal deposition in all-solid-state lithium sulfur batteries with polymer-in-salt polysiloxane electrolyte. *Energy Storage Mater.* **2018**, *15*, 37–45. [CrossRef]

41. Zhang, J.; Si, Y.; Huang, Q.; Yang, T.; Wang, C.; Ji, K.; Wang, J.; Chen, M. Gradient distribution of functional components in PAN-based electrolytes to endow solid-state lithium sulfur batteries with long cycle life. *Sustain. Energy Fuels* **2022**, *6*, 4240–4247. [CrossRef]

42. Liu, M.; Jiang, H.R.; Ren, Y.X.; Zhou, D.; Kang, F.Y.; Zhao, T.S. In-situ Fabrication of a Freestanding Acrylate-based Hierarchical Electrolyte for Lithium-sulfur Batteries. *Electrochim. Acta* **2016**, *213*, 871–878. [CrossRef]

43. Aldalur, I.; Zhang, H.; Piszcz, M.; Oteo, U.; Rodriguez-Martinez, L.M.; Shanmukaraj, D.; Rojo, T.; Armand, M. Jeffamine® based polymers as highly conductive polymer electrolytes and cathode binder materials for battery application. *J. Power Sources* **2017**, *347*, 37–46. [CrossRef]

44. Zhou, J.; Ji, H.; Liu, J.; Qian, T.; Yan, C. A new high ionic conductive gel polymer electrolyte enables highly stable quasi-solid-state lithium sulfur battery. *Energy Storage Mater.* **2019**, *22*, 256–264. [CrossRef]

45. Yang, W.; Yang, W.; Feng, J.; Ma, Z.; Shao, G. High capacity and cycle stability Rechargeable Lithium–Sulfur batteries by sandwiched gel polymer electrolyte. *Electrochim. Acta* **2016**, *210*, 71–78. [CrossRef]

46. Song, J.; Noh, H.; Lee, H.; Lee, J.-N.; Lee, D.J.; Lee, Y.; Kim, C.H.; Lee, Y.M.; Park, J.-K.; Kim, H.-T. Polysulfide rejection layer from alpha-lipoic acid for high performance lithium–sulfur battery. *J. Mater. Chem. A* **2015**, *3*, 323–330. [CrossRef]

47. Han, D.-D.; Liu, S.; Liu, Y.-T.; Zhang, Z.; Li, G.-R.; Gao, X.-P. Lithiophilic gel polymer electrolyte to stabilize the lithium anode for a quasi-solid-state lithium–sulfur battery. *J. Mater. Chem. A* **2018**, *6*, 18627–18634. [CrossRef]

48. Liu, M.; Zhou, D.; He, Y.-B.; Fu, Y.; Qin, X.; Miao, C.; Du, H.; Li, B.; Yang, Q.-H.; Lin, Z.; et al. Novel gel polymer electrolyte for high-performance lithium–sulfur batteries. *Nano Energy* **2016**, *22*, 278–289. [CrossRef]

49. Du, H.; Li, S.; Qu, H.; Lu, B.; Wang, X.; Chai, J.; Zhang, H.; Ma, J.; Zhang, Z.; Cui, G. Stable cycling of lithium-sulfur battery enabled by a reliable gel polymer electrolyte rich in ester groups. *J. Membr. Sci.* **2018**, *550*, 399–406. [CrossRef]

50. Yang, Y.J.; Wang, R.; Xue, J.X.; Liu, F.Q.; Yan, J.; Jia, S.X.; Xiang, T.Q.; Huo, H.; Zhou, J.J.; Li, L. In situ forming asymmetric bi-functional gel polymer electrolyte in lithium–sulfur batteries. *J. Mater. Chem. A* **2021**, *9*, 27390–27397. [CrossRef]

51. Jiang, Y.; Li, F.; Mei, Y.; Ding, Y.; Pang, H.; Zhang, P. Gel polymer electrolyte based on hydrophilic–lipophilic TiO_2-modified thermoplastic polyurethane for high-performance Li-ion batteries. *J. Mater. Sci.* **2020**, *56*, 2474–2485. [CrossRef]

52. Karim, J.; Aminah Mohd Noor, S.; Zuliana Dzulkipli, M.; Ahmad, A.; Sukor Su'ait, M.; Hasyareeda Hassan, N. Influence of Electron beam radiation on the properties of Surface-Modified Titania-Filled gel polymer electrolytes using vinyltriethoxysilane (VTES) for lithium battery application. *Results Chem.* **2022**, *4*, 100383. [CrossRef]

53. Guo, J.; Chen, Y.; Xiao, Y.; Xi, C.; Xu, G.; Li, B.; Yang, C.; Yu, Y. Flame-retardant composite gel polymer electrolyte with a dual acceleration conduction mechanism for lithium ion batteries. *Chem. Eng. J.* **2021**, *422*, 130526. [CrossRef]

54. Ahn, J.H.; You, T.-S.; Lee, S.-M.; Esken, D.; Dehe, D.; Huang, Y.-C.; Kim, D.-W. Hybrid separator containing reactive, nanostructured alumina promoting in-situ gel electrolyte formation for lithium-ion batteries with good cycling stability and enhanced safety. *J. Power Sources* **2020**, *472*, 228519. [CrossRef]

55. Wu, F.; Chen, N.; Chen, R.; Wang, L.; Li, L. Organically modified silica-supported ionogels electrolyte for high temperature lithium-ion batteries. *Nano Energy* **2017**, *31*, 9–18. [CrossRef]

56. Li, Y.J.; Guo, C.; Yue, L.S.; Qu, W.J.; Chen, N.; Dai, Y.-J.; Chen, R.-J.; Wu, F. Organosilicon-group-derived silica-ionogel electrolyte for lithium ion batteries. *Rare Met.* **2018**, *37*, 504–509. [CrossRef]

57. Li, X.; Li, S.; Zhang, Z.; Huang, J.; Yang, L.; Hirano, S.i. High-performance polymeric ionic liquid–silica hybrid ionogel electrolytes for lithium metal batteries. *J. Mater. Chem. A* **2016**, *4*, 13822–13829. [CrossRef]

58. Lin, Y.Y.; Chen, Y.M.; Hou, S.S.; Jan, J.S.; Lee, Y.L.; Teng, H. Diode-like gel polymer electrolytes for full-cell lithium ion batteries. *J. Mater. Chem. A* **2017**, *5*, 17476–17481. [CrossRef]

59. Pei, F.; Dai, S.; Guo, B.; Xie, H.; Zhao, C.; Cui, J.; Fang, X.; Chen, C.; Zheng, N. Titanium–oxo cluster reinforced gel polymer electrolyte enabling lithium–sulfur batteries with high gravimetric energy densities. *Energy Environ. Sci.* **2021**, *14*, 975–985. [CrossRef]

60. Xie, P.; Yang, R.; Zhou, Y.; Zhang, B.; Tian, X. Rationally designing composite gel polymer electrolyte enables high sulfur utilization and stable lithium anode. *Chem. Eng. J.* **2022**, *450*, 138195. [CrossRef]

61. Jiang, H.; Han, Y.; Wang, H.; Zhu, Y.; Guo, Q.; Jiang, H.; Zheng, C.; Xie, K. LiS-LiPS (LPS) Composite Synthesized by Liquid-Phase Shaking for All-Solid-State Lithium-Sulfur Batteries with High Performance. *Energy Technol.* **2020**, *8*, 2000023. [CrossRef]

62. Hakari, T.; Hayashi, A.; Tatsumisago, M. LiS-Based Solid Solutions as Positive Electrodes with Full Utilization and Superlong Cycle Life in All-Solid-State Li/S Batteries. *Adv. Sustain. Syst.* **2017**, *1*, 1700017. [CrossRef]

63. Phuc, N.H.H.; Takaki, M.; Kazuhiro, H.; Hiroyuki, M.; Atsunori, M. Dual effect of MgS addition on LiS ionic conductivity and all-solid-state Li–S cell performance. *SN Appl. Sci.* **2020**, *2*, 1803. [CrossRef]

64. Gamo, H.; Maeda, T.; Hikima, K.; Deguchi, M.; Fujita, Y.; Kawasaki, Y.; Sakuda, A.; Muto, H.; Phuc, N.H.H.; Hayashi, A.; et al. Synthesis of an AlI-doped LiS positive electrode with superior performance in all-solid-state batteries. *Mater. Adv.* **2022**, *3*, 2488–2494. [CrossRef]

65. Lin, Z.; Liu, Z.; Dudney, N.J.; Liang, C. Lithium Superionic Sulfide Cathode for All-Solid Lithium-Sulfur Batteries. *ACS Nano* **2013**, *7*, 2829–2833. [CrossRef] [PubMed]

66. Long, L.; Wang, S.; Xiao, M.; Meng, Y. Polymer electrolytes for lithium polymer batteries. *J. Mater. Chem. A* **2016**, *4*, 10038–10069. [CrossRef]

67. Wang, Z.; Chen, S.; Huang, Z.; Wei, Z.; Shen, L.; Gu, H.; Xu, X.; Yao, X. High conductivity polymer electrolyte with comb-like structure via a solvent-free UV-cured method for large-area ambient all-solid-sate lithium batteries. *J. Mater.* **2019**, *5*, 195–203. [CrossRef]

68. Jayathilaka, P.; Dissanayake, M.; Albinsson, I.; Mellander, B.-E. Effect of nano-porous AlO on thermal, dielectric and transport properties of the (PEO) LiTFSI polymer electrolyte system. *Electrochim. Acta* **2002**, *47*, 3257–3268. [CrossRef]

69. Watanabe, M.; Endo, T.; Nishimoto, A.; Miura, K.; Yanagida, M. High ionic conductivity and electrode interface properties of polymer electrolytes based on high molecular weight branched polyether. *J. Power Source* **1999**, *81–82*, 786–789. [CrossRef]

70. Kim, S.-C.; Oh, T.H.; Kim, D.W.; Lee, C.; Kang, Y. Ion-conducting hyperbranched PEG electrolytes derived from poly(glycidol). *Macromol. Res.* **2009**, *17*, 141–143. [CrossRef]

71. Imholt, L.; Dörr, T.S.; Zhang, P.; Ibing, L.; Cekic-Laskovic, I.; Winter, M.; Brunklaus, G. Grafted polyrotaxanes as highly conductive electrolytes for lithium metal batteries. *J. Power Source* **2019**, *409*, 148–158. [CrossRef]

72. Song, Y.X.; Shi, Y.; Wan, J.; Lang, S.-Y.; Hu, X.C.; Yan, H.J.; Liu, B.; Guo, Y.G.; Wen, R.; Wan, L.J. Direct tracking of the polysulfide shuttling and interfacial evolution in all-solid-state lithium–sulfur batteries: A degradation mechanism study. *Energy Environ. Sci.* **2019**, *12*, 2496–2506. [CrossRef]

73. Borodin, O.; Smith Grant, D. Mechanism of Ion Transport in Amorphous Poly(ethylene oxide)/LiTFSI from Molecular Dynamics Simulations. *Macromolecules* **2006**, *39*, 1620–1629. [CrossRef]

74. Stolwijk, N.A.; Heddier, C.; Reschke, M.; Wiencierz, M.; Bokeloh, J.; Wilde, G. Salt-Concentration Dependence of the Glass Transition Temperature in PEO–NaI and PEO–LiTFSI Polymer Electrolytes. *Macromolecules* **2013**, *46*, 8580–8588. [CrossRef]

75. Marceau, H.; Kim, C.-S.; Paolella, A.; Ladouceur, S.; Lagacé, M.; Chaker, M.; Vijh, A.; Guerfi, A.; Julien, C.M.; Mauger, A.; et al. In operando scanning electron microscopy and ultraviolet–visible spectroscopy studies of lithium/sulfur cells using all solid-state polymer electrolyte. *J. Power Sources* **2016**, *319*, 247–254. [CrossRef]

76. Fang, R.; Xu, H.; Xu, B.; Li, X.; Li, Y.; Goodenough, J.B. Reaction Mechanism Optimization of Solid-State Li–S Batteries with a PEO-Based Electrolyte. *Adv. Funct. Mater.* **2020**, *31*, 2001812. [CrossRef]

77. Sheng, O.; Jin, C.; Luo, J.; Yuan, H.; Fang, C.; Huang, H.; Gan, Y.; Zhang, J.; Xia, Y.; Liang, C.; et al. Ionic conductivity promotion of polymer electrolyte with ionic liquid grafted oxides for all-solid-state lithium–sulfur batteries. *J. Mater. Chem. A* **2017**, *5*, 12934–12942. [CrossRef]

78. Wei, B.; Huang, S.; Song, Y.; Wang, X.; Liu, M.; Jin, H.; Cao, G. A three-in-one C60-integrated PEO-based solid polymer electrolyte enables superior all-solid-state lithium–sulfur batteries. *J. Mater. Chem. A* **2023**, *11*, 11426–11435. [CrossRef]

79. Liu, S.M.; Chen, M.X.; Xie, Y.; Liu, D.H.; Zheng, J.F.; Xiong, X.; Jiang, H.; Wang, L.C.; Luo, H.; Han, K. Nb_2CT_x MXene boosting PEO polymer electrolyte for all-solid-state Li-S batteries: Two birds with one stone strategy to enhance Li^+ conductivity and polysulfide adsorptivity. *Rare Met.* **2023**, *42*, 2562–2576. [CrossRef]

80. Zhang, X.; Zhang, H.; Geng, Y.; Shi, Z.; Zhu, S.; Xu, Q.; Min, Y. A multifunctional nano filler for solid polymer electrolyte toward stable cycling for lithium-metal anodes in lithium–sulfur batteries. *Chem. Eng. J.* **2022**, *444*, 136328. [CrossRef]

81. Wang, P.F.; He, X.; Lv, Z.C.; Song, H.; Song, X.; Yi, T.F.; Xu, N.; He, P.; Zhou, H. Light-Driven Polymer-Based All-Solid-State Lithium-Sulfur Battery Operating at Room Temperature. *Adv. Funct. Mater.* **2023**, *33*, 2211074. [CrossRef]

82. Song, X.; Wang, M.; Wang, S.; Cheng, Z.; Zhang, T.; Zhu, T.; Song, H.; Yu, L.; Xu, J.; Chen, K. A wide temperature solid-state Li–S battery enabled by a plasmon-enhanced copper–silicon nanowire photothermal current collector. *J. Mater. Chem. A* **2022**, *10*, 22584–22591. [CrossRef]

83. Li, M.; Frerichs, J.E.; Kolek, M.; Sun, W.; Zhou, D.; Huang, C.J.; Hwang, B.J.; Hansen, M.R.; Winter, M.; Bieker, P. Solid-State Lithium–Sulfur Battery Enabled by Thio-LiSICON/Polymer Composite Electrolyte and Sulfurized Polyacrylonitrile Cathode. *Adv. Funct. Mater.* **2020**, *30*, 191023. [CrossRef]

84. Zhong, L.; Wang, S.; Xiao, M.; Liu, W.; Han, D.; Li, Z.; Qin, J.; Li, Y.; Zhang, S.; Huang, S.; et al. Addressing interface elimination: Boosting comprehensive performance of all-solid-state Li-S battery. *Energy Storage Mater.* **2021**, *41*, 563–570. [CrossRef]

85. Gao, J.; Sun, C.; Xu, L.; Chen, J.; Wang, C.; Guo, D.; Chen, H. Lithiated Nafion as polymer electrolyte for solid-state lithium sulfur batteries using carbon-sulfur composite cathode. *J. Power Source* **2018**, *382*, 179–189. [CrossRef]